World Academy of Science, Engineering and Technology
International Journal of Mechanical and Mechatronics Engineering
Vol:11, No:7, 2017

# Failure Criterion for Mixed Mode Fracture of Cracked Wood Specimens

Mahdi Fakoor, Seyed Mohammad Navid Ghoreishi



***Abstract*—**Investigation of fracture of wood components can prevent from catastrophic failures. Created fracture process zone (FPZ) in crack tip vicinity has important effect on failure of cracked composite materials. In this paper, a failure criterion for fracture investigation of cracked wood specimens under mixed mode I/II loading is presented. This criterion is based on maximum strain energy release rate and material nonlinearity in the vicinity of crack tip due to presence of microcracks. Verification of results with available experimental data proves the coincidence of the proposed criterion with the nature of fracture of wood. To simplify the estimation of nonlinear properties of FPZ, a damage factor is also introduced for engineering and application purposes.

***Keywords*—**Fracture criterion, mixed mode loading, damage zone, microcracks.

## I. Introduction

WOOD is a natural, heterogeneous, anisotropic, hygroscopic composite material with cellular structure. This natural structure dictates strongly directional dependent properties. Wood is extremely mechanically efficient compared to most other materials, due to the high strength and stiffness relating to its weight [1]. Nowadays, large dimension wood structures are developed in different modern civil structures [2]. Also, wood can be produced from natural renewable sources without any complicated manufacturing process.

Cracks in wood structures are usually available due to inherent defects or production process [1]. These cracked structures often are subjected to various loading conditions. Most probable load situation which may lead to fracture of wood structures is mixed mode I/II loading.

Fracture phenomenon of wood is associated with a significant process zone [3]. The created damage zone is often in the form of bridging or microcracks and can prevent from catastrophic fracture of wooden structures due to consumption of energy.

Although the presence of microcracks in the vicinity of crack tip will improve fracture properties of wood, it also causes to some difficulties and complicacies in the analysis and investigation of fracture phenomenon. To estimate a good approximation and applicable model for wood fracture process, a calculation of the microcrack distribution and a change in the compliance of material in FPZ are necessary. Since the mechanisms responsible for wood fracture are numerous and complex, formulating of a strict and practical model appears to be very difficult and has not been published yet. Because of these difficulties, curve fitting approach has been employed by some researches, which needs significant number of experimental data. A mixed mode fracture criterion is proposed by Mall and Murphy [4]. Significant researches have been done by Wu on Balsa wood center notch specimens [5]. Wu has an interactive experimental mixed mode criterion which is widely used for composite structures. This empirical criterion contains two experimental coefficients, which makes it difficult to use.

Another approach for the presentation of mixed mode I/II fracture criterion is the extension of well-known available fracture criteria in to composite materials. Jernkvist was the first researcher who has extended Maximum Strain Energy Release Rate (MSER) [6] and Minimum Strain Energy Density (MSED) criteria [7], in to wooden structures [8]. He used these common isotropic fracture criteria and this experimental observation where cracks in wood components are propagated along the fibers, for any crack-fiber inclinations. He suggested two criteria for orthotropic materials based on MSER and MSED criteria with assumption of self-similar crack propagation. His results are too conservative and are not verified with experimental data [9]. Neglecting the effect of wasted energy in FPZ may be the main reason for this deficiency. Maximum Principal Stress (MPS) criterion is also extended for cracked composite materials which contained better results [9].

Nature of FPZ and nonlinear behaviour of this region are also studied by some researchers separately without paying attention to the presentation of a fracture criterion. Vasic and Smith [3] found the significance of FPZ effects on fracture behavior of wood specimens. They proposed bridging crack [10] and lattice fracture approach [10] based on Hillerborg's model [11].

In this paper, we will first show that the stress based criteria which are material independent (always Poisson's ratio) are not able to predict the material nonlinearity effects in FPZ. Therefore, one of the main objectives of this article is to modify the energy based mixed mode criteria, which are material dependent, in order to consider the effects of energy wasted by micro crack formation in FPZ surrounded around the crack tip. By extraction of mechanical properties of damage zone, modified maximum strain energy release rate criterion is introduced with real elastic properties of FPZ. Scots pine and Norway spruce mixed mode experimental

Mahdi Fakoor is with the Faculty of New Sciences and Technologies, University of Tehran, Tehran, Iran (phone: +98 21 61118597; fax: +98 21 88057915; e-mail: mfakoor@ut.ac.ir).

Seyed Mohammad Navid Ghoreishi is with the Faculty of New Sciences and Technologies, University of Tehran, Tehran, Iran (e-mail: navid_ghoreishi@ut.ac.ir).

fracture data, previously polished in [12] and [9] respectively, will be used for the results verification of the suggested criterion. To use this criterion in applied and practical engineering goals, a damage factor is introduced to simplify the estimation of damage zone mechanical properties. It is found that this damage factor does not depend on wood species, but is strongly dependent on wood crack propagation plane system. Therefore, the modified energy criterion can be easily used for fracture behavior prediction of wood specimens.

## II. Model Description and Material Properties

Wood is a cylindrically orthotropic material which has unique mechanical properties in the directions of three mutually perpendicular axes:

- Longitudinal (L) which is parallel to the fibers,
- Radial (R), which is normal to the growth rings and
- Tangential (T), which is is perpendicular to the grain.

These axes are shown in Fig. 1 [13]. A crack may lie in one of these three planes. This gives six crack-propagation systems, RL, TL, LR, TR, LT, and RT, as shown in Fig. 2. Of these crack propagation systems, RL, TL, TR, and RT are most probable for crack extension.

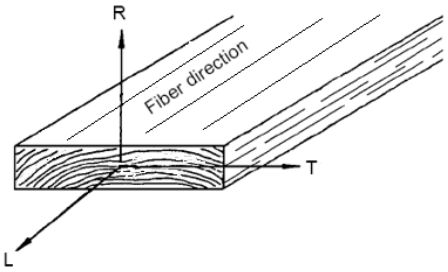


Fig. 1 Principal axes of orthotropy (R, T, L) in a tree trunk

Cracks in RL and TL orientations are the most probable defects due to low strength and stiffness of wood perpendicular to the grain.

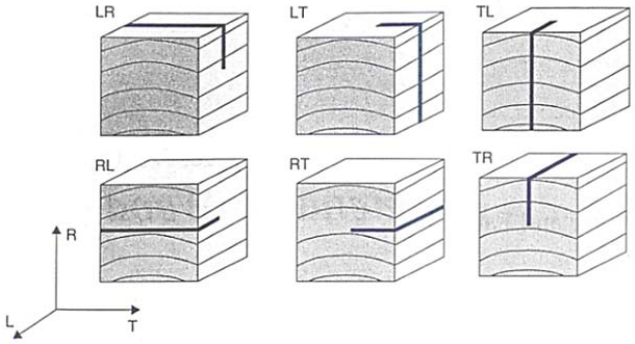


Fig. 2 Possible crack propagation systems for wood [1]

In this article, mixed mode fracture is studied in the RL plane strain system. The configuration of analyzed specimen and crack tip coordinate system are shown in Fig. 3, where x-axis corresponds to the wood longitudinal (L) direction and "y" is R direction.

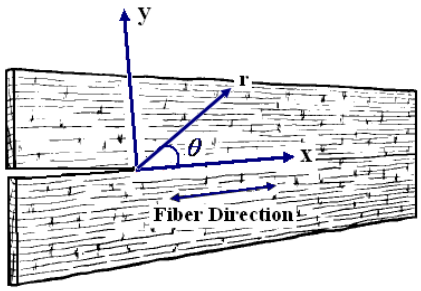


Fig. 3 Possible crack propagation systems for wood [1]

Scots pine, Norway spruce, Red spruce, and Hemlock western are four well known wood species that are used in this study. The elastic properties of these materials are summarized in Table I.

TABLE I
Elastic Properties of Scots Pine, Norway Spruce, Red Spruce and Hemlock Western Wood Applied in the Analysis

| Parameter | Norway spruce | Scots pine | Douglas fir | Hemloak Western |
|---|---|---|---|---|
| $E_R\ (GPa)$ | 0.81 | 1.10 | 0.92 | 0.31 |
| $E_T\ (GPa)$ | 0.64 | 0.57 | 0.68 | 0.58 |
| $E_L\ (GPa)$ | 11.84 | 16.3 | 13.6 | 10.1 |
| $G_{RL}\ (GPa)$ | 0.63 | 1.74 | 0.87 | 0.32 |
| $\upsilon_{LR}$ | 0.38 | 0.47 | 0.29 | 0.42 |
| $\upsilon_{LT}$ | 0.56 | 0.45 | 0.45 | 0.48 |
| $\upsilon_{TR}$ | 0.34 | 0.31 | 0.37 | 0.38 |
| $K_{IC}^{RL}\left(MPa.m^{0.5}\right)$ | 0.58 | 0.49 | 0.36 | 0.37 |
| $K_{IIC}^{RL}\left(MPa.m^{0.5}\right)$ | 1.52 | 1.32 | 2.23 | 2.24 |

## III. Calculation of FPZ Properties

In this section, wasted energy by microcracks which is proposed in [14] is considered for the calculation of mechanical properties of FPZ. Therefore, the fracture of wood specimens will be modeled accurately, by employing these damage properties in maximum strain energy release rate criterion.

An uncracked isotropic solid under uniform hydrostatic stress p is shown in Fig. 4. The absorbed potential energy by the aforementioned body could be written as:

$$\phi=\frac{V}{2}(\sigma_{xx}\varepsilon_{xx}+\sigma_{yy}\varepsilon_{yy}+\sigma_{zz}\varepsilon_{zz})=\frac{-VP}{2}(\varepsilon_{xx}+\varepsilon_{yy}+\varepsilon_{zz}) \quad (1)$$

in which $V$ is the total volume, and $K$ is the bulk modulus of the material shown in Fig. 4, which is given by:

$$K=\frac{Volumetric\ \ Stress}{Volumetric\ \ Strain}=\frac{P}{\varepsilon_{xx}+\varepsilon_{yy}+\varepsilon_{zz}} \quad (2)$$

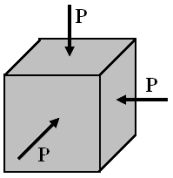


Fig. 4 Isotropic body under hydrostatic pressure

Potential energy of un-cracked body could be rewritten as follows utilizing (2) based on the definition of bulk modulus as:

$$\phi = -\frac{P^2 V}{2K} \tag{3}$$

Considering a set of cracks in the mentioned solid will change the energy balance as [14]:

$$-\frac{P^2 V}{2\bar{K}} = -\frac{P^2 V}{2K} + \Delta\varphi \tag{4}$$

In which, $\Delta\phi$ is the change in potential energy. $\bar{K}$ is the bulk modulus of the cracked material.

By dimensional analysis, the wasted energy due to one microcrack must have the following form [14]:

$$G = \frac{P^2 a^3}{\bar{E}} f(\bar{\nu}) \tag{5}$$

where $a$ is the crack dimension; $\bar{E}$ is the modulus of elasticity of the cracked body; $\bar{\nu}$ is its effective Poisson's ratio; and $f$ is a non-dimensional shape factor. Therefore, the energy change due to $N$ microcracks is given by [14]:

$$\Delta\phi = -\frac{P^2}{E}\sum a^3 f(\bar{\nu}) \tag{6}$$

Substituting into (5) and considering the following standard relation:

$$\frac{\bar{E}}{\bar{K}} = 3(1-2\bar{\nu}) \tag{7}$$

We will have [14]:

$$\frac{\bar{K}}{K} = 1 - \frac{2N\langle a^3 f(\bar{\nu})\rangle}{3(1-2\bar{\nu})} \tag{8}$$

where angle brackets show the average values. If crack size and shape are considered to be uncorrelated, (8) can be replaced by:

$$\frac{\bar{K}}{K} = 1 - \frac{2N\langle a^3\rangle\langle f(\bar{\nu})\rangle}{3(1-2\bar{\nu})} \tag{9}$$

In the case of uniaxial tension $s$ (Fig. 5) which is applied to a cracked body, the energy balance could be as:

$$-\frac{s^2 V}{2\bar{E}} = -\frac{s^2 V}{2E} + \Delta\phi \tag{10}$$

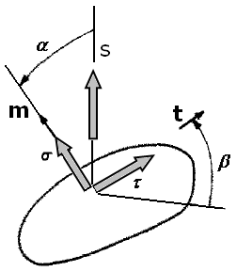


Fig. 5 Plane crack and resolved stresses [14]

Considering $\sigma$ and $\tau$ as normal and tangential stresses in the plane of the crack respectively, we have [14]:

$$G = \frac{a^3}{\bar{E}}\left[\sigma^2 f(\bar{\nu}) + \tau^2 g(\bar{\nu},\beta)\right] \tag{11}$$

Here, $g(\bar{\nu},\beta)$ is another non-dimensional shape factor. $\sigma$ and $\tau$ can be written versus $s$ (see Fig. 5) as:

$$\begin{aligned}\sigma &= s\cos^2\alpha \\ \tau &= s\sin\alpha\cos\alpha\end{aligned} \tag{12}$$

Summing (11) over all cracks to get $-\Delta\phi$, and substituting into (10) gives:

$$\frac{\bar{E}}{E} = 1 - 2N\left\langle a^3\left(f(\bar{\nu})\cos^4\alpha + g(\bar{\nu},\beta)\sin^2\alpha\cos^2\alpha\right)\right\rangle \tag{13}$$

In [14], crack sizes, shapes, and orientations are assumed to be uncorrelated. Utilizing the following relations and uncorrelated assumption:

$$\begin{aligned}\langle\cos^4\alpha\rangle &= \frac{1}{5} \\ \langle\sin^2\alpha\cos^2\alpha\rangle &= \frac{2}{15}\end{aligned} \tag{14}$$

Equation (13) could be rewritten as:

$$\frac{\bar{E}}{E} = 1 - \frac{2N\langle a^3\rangle}{15}\left[3\langle f(\bar{\nu})\rangle + 2\langle g(\bar{\nu},\beta)\rangle\right] \tag{15}$$

Equations (9) and (15), together with (8), provide simultaneous equations for the determination of $\bar{K}$, $\bar{E}$, and $\bar{\nu}$ and also any other related elastic constants (such as the shear modulus $\bar{G}$).

Crack energy and $f(\bar{\nu})$ and $g(\bar{\nu},\beta)$ functions are calculated in [14] for several crack shapes in detail. For example, for a solid with elliptic cracks as shown in Fig. 6, we have:

$$f(\bar{\nu}) = \left(\frac{4\pi}{3}\right)\left(\frac{b}{a}\right)^2\left(\frac{1-\bar{\nu}^2}{E(k)}\right) \tag{16}$$

and

$$g(\bar{\nu},\beta)=\frac{4\pi}{3}\left(\frac{b}{a}\right)^2(1-\bar{\nu}^2)[R(k,\bar{\nu})\cos^2\beta+Q(k,\bar{\nu})\sin^2\beta] \quad (17)$$

in which

$$\begin{aligned} R(k,\nu)&=k^2[(k^2-\nu)E(k)+\nu k_1^2\mathbf{K}(k)]^{-1}\\ Q(k,\nu)&=k^2[(k^2+\nu k_1^2)E(k)-\nu k_1^2\mathbf{K}(k)]^{-1}\end{aligned} \quad (18)$$

$E(k)$ is the complete elliptic integral of the second kind, and $\mathbf{K}(k)$ is the complete elliptic integral of the first kind.

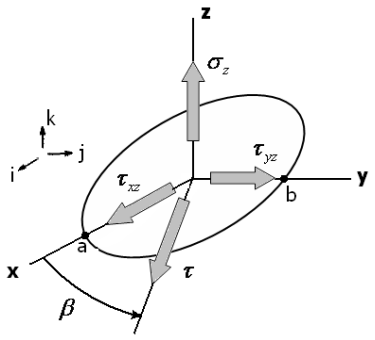


Fig. 6 Elliptic crack and resolved stresses [14]

Under the simplifying assumption that all the cracks are elliptic and have the same aspect ratio $b/a$, (16) is changed to:

$$\langle f(\bar{\nu})\rangle=\left(\frac{4\pi}{3}\right)\left\langle\frac{b}{a}\right\rangle^2\left(\frac{1-\bar{\nu}^2}{E(k)}\right) \quad (19)$$

Substituting in (13):

$$\frac{\bar{K}}{K}=1-\frac{8\pi N\langle ab^2\rangle(1-\bar{\nu}^2)}{9(1-2\bar{\nu})E(k)} \quad (20)$$

Assuming crack area, $A=\pi ab$, and $P=4aE(k)$ as crack surrounding space, crack-density parameter $\varepsilon$ is defined by:

$$\varepsilon=\frac{2N}{\pi}\left\langle\frac{A^2}{P}\right\rangle \quad (21)$$

So that (20) can be rewritten in its final form

$$\frac{\bar{K}}{K}=1-\frac{16}{9}\left(\frac{1-\bar{\nu}^2}{1-2\bar{\nu}}\right)\varepsilon \quad (22)$$

For fixed $b/a$ ratio and considering $\langle\cos^2\beta\rangle=\langle\sin^2\beta\rangle=1/2$, from (17) for $\langle g(\bar{\nu},\beta)\rangle$ we have:

$$\langle g(\bar{\nu},\beta)\rangle=\frac{2\pi}{3}\left(\frac{b}{a}\right)^2(1-\bar{\nu}^2)[R(k,\bar{\nu})+Q(k,\bar{\nu})] \quad (23)$$

Substituting $\langle f(\bar{\nu})\rangle$ and $\langle g(\bar{\nu},\beta)\rangle$ in (15)

$$\frac{\bar{E}}{E}=1-\frac{16(1-\bar{\nu}^2)}{45}\left[3+T\left(\frac{b}{a},\bar{\nu}\right)\right]\varepsilon \quad (24)$$

where [14]:

$$\begin{aligned} T\left(\frac{b}{a},\bar{\nu}\right)&=E(k)\left[R(k,\bar{\nu})+Q(k,\bar{\nu})\right]=k^2E(k)\\ &\times\left\{[(k^2-\bar{\nu})E(k)+\bar{\nu}k_1^2\mathbf{K}(k)]^{-1}+[(k^2+\bar{\nu}k_1^2)E(k)-\bar{\nu}k_1^2\mathbf{K}(k)]^{-1}\right\}\end{aligned} \quad (25)$$

The standard relation (8) among $\bar{K}$, $\bar{E}$ and $\bar{\nu}$, and the similar one for $K$, $E$, and $\nu$, can be combined to [14]:

$$2(\nu-\bar{\nu})=(1-2\bar{\nu})\left(1-\frac{\bar{K}}{K}\right)-(1-2\nu)\left(1-\frac{\bar{E}}{E}\right) \quad (26)$$

Substituting (22) and (24) in (36)

$$\varepsilon=\frac{45}{8}\frac{\nu-\bar{\nu}}{(1-\bar{\nu}^2)[2(1+3\nu)-(1-2\nu)T]} \quad (27)$$

To round out the results for $\bar{K}/K$ and $\bar{E}/E$, an analogous expression for $\bar{G}/G$ is easily found from standard elastic relations. Since $1/G-3/E+1/3K=0$, and similarly for the barred quantities, it follows that

$$2\left(1-\frac{\bar{G}}{G}\right)(1+\bar{\nu})-3\left(1-\frac{\bar{E}}{E}\right)+(1-2\bar{\nu})\left(1-\frac{\bar{K}}{K}\right)=0 \quad (28)$$

where

$$\frac{\bar{G}}{G}=1-\frac{32}{45}(1-\bar{\nu})\left[1+\frac{3}{4}T\left(\frac{b}{a},\bar{\nu}\right)\right]\varepsilon \quad (29)$$

An independent calculation of $\bar{G}/G$ by a direct procedure to that used for finding $\bar{E}/E$ gives the same answer.

It can be easily shown that for circular cracks $(b/a=1)$, $T=4/(2-\bar{\nu})$ and $\varepsilon=N\langle a^3\rangle$, and (24) and (29) are reduced to [14]:

$$\frac{\bar{E}}{E}=1-\frac{16}{45}\frac{(1-\bar{\nu}^2)(10-3\bar{\nu})}{(2-\bar{\nu})}\varepsilon \quad (30)$$

$$\frac{\bar{G}}{G}=1-\frac{32}{45}\frac{(1-\bar{\nu})(5-\bar{\nu})}{(2-\bar{\nu})}\varepsilon \quad (31)$$

Also for the limiting case of long narrow elliptic cracks $(b/a\to 0)$, with $T=(2-\bar{\nu})/(1-\bar{\nu})$ and $\varepsilon=(\pi/2)N\langle ab^2\rangle$, the results reduced to:

$$\frac{\bar{E}}{E}=1-\frac{16}{45}(1+\bar{\nu})(5-4\bar{\nu})\varepsilon \quad (32)$$

$$\frac{\bar{G}}{G}=1-\frac{8}{45}(10-7\bar{\nu})\varepsilon \tag{33}$$

## IV. Modification of Energy Based Criterion

Based on the above analysis, variations of mechanical properties for investigated wood species in FPZ are shown in Fig. 7 versus crack density parameter.

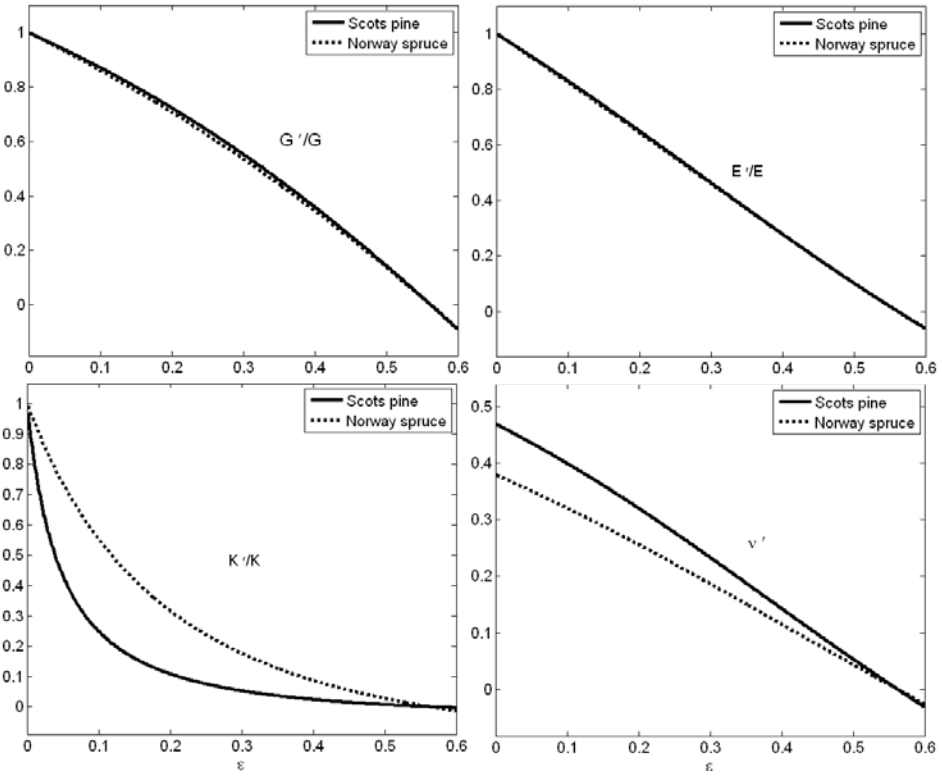


Fig. 7 Effective mechanical properties in damage zone in the vicinity of crack tip

As we can see, $\bar{\nu},\bar{E},\bar{G}$, and $\bar{K}$ are decreasing functions of $\varepsilon$ and they also tend to zero at critical crack density parameter $\varepsilon=0.56$ for all kinds of investigated wood. This vanishing of the moduli can be interpreted as a loss of coherence of the material that is produced by an intersecting crack network at the critical value 9/16 of the crack density parameter. It can be shown that the unstable crack growth starts at $\varepsilon=0.4$, and at $\varepsilon=0.56$, the FPZ will be portion of the main crack; in the other words, the specimen in fracture process will completely tear apart and the load capacity in this region is vanished.

Now, we can use maximum strain energy release rate criterion with effective material properties in FPZ. As explained earlier in detail, this procedure will help us to simulate the crack propagation process in wood damaged matrix actually. Therefore, the required energy for formation and growth of microcracks is considered in our calculations. So, the maximum strain energy release rate criterion is modified as follows:

$$K_I^2+\rho_c K_{II}^2-K_{Ic}=0 \tag{34}$$

The authors introduce $\rho_c$ as a "compliance damage factor".

$$\rho_c=\left(C'_{11}/C'_{22}\right)^{1/2}_{damaged} \tag{35}$$

Fracture limit curves using compliance softening factor $\rho_c$ is plotted in Figs. 8 and 9 for Scots pine and Norway spruce wood, respectively. This factor increases the compliance of representative volume element damage zone and therefore the area under fracture limit curve in $K_I-K_{II}$ coordinate.

It can be found from Figs. 8 and 9 that considering the portion of energy that causing microcrack formation and growth in FPZ justifies the difference between the linear fracture approximation and experimental data. The discrepancy between modified criterion and experimental data for Scots pine wood is too small and for Norway spruce is less than 10%, which is very good agreement.

## V.A Simple Method for Calculation of Damage Factor (Toughness Approach)

In this section, a simple method will be presented to avoid complicated calculation of material properties in FPZ. This simple method is based on definition of a damage factor in order to release (3) from damage parameters. In the other words, dissipative mechanisms and wasted energy by microcracks are modeled in maximum strain energy release

rate criterion by a suitable damage factor. The released energy due to microcrack formation and growth is in fact the marked area, between two fracture curves, that is shown in Figs. 10 and 11.

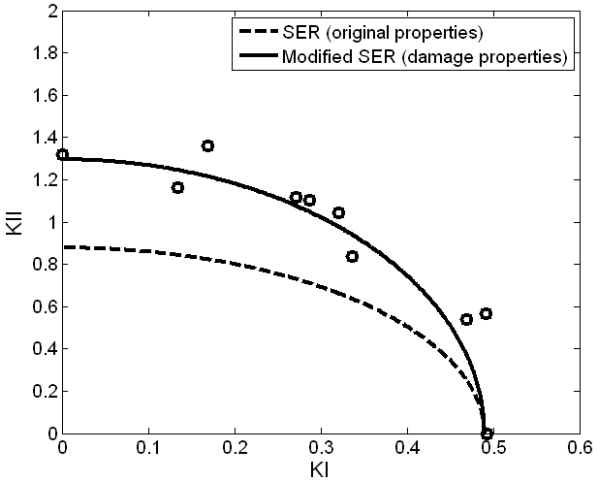


Fig. 8 Fracture limit curves for strain energy release rate (SER) criterion considering linear and nonlinear behavior of material in FPZ, in comparison with experimental data for Scots pine wood [12]

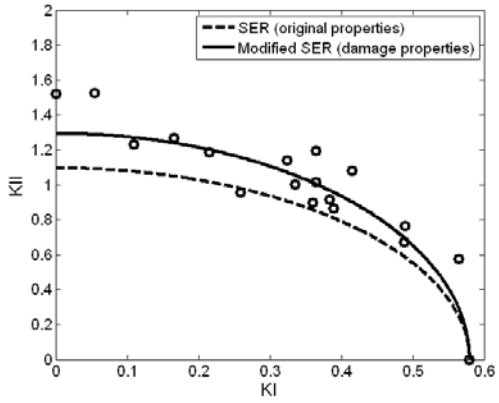


Fig. 9 Fracture limit curves for modified strain energy release rate criterion considering linear and nonlinear behavior of material in FPZ, in comparison with experimental data for Norway spruce [9]

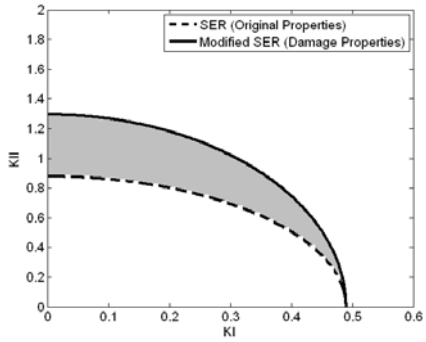


Fig. 10 Difference between fracture curves in linear and non-linear approach for Scots pine wood

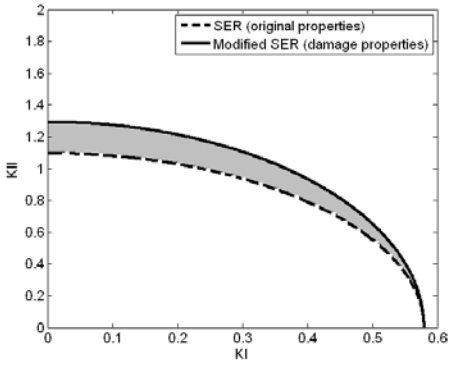


Fig. 11 Difference between fracture curves in linear and non-linear approach for Norway spruce wood

With more detailed investigation of maximum strain energy release rate criterion, it can be found that the $\alpha_3$ factor, defined in this criterion, is dependent on elastic compliance matrix of material, and this dependency is the main reason for dissatisfaction of pure mode II boundary condition. It can be easily shown that, for satisfaction of pure mode II condition in maximum strain energy release rate criterion, the following mode II damage, *D* factor must be used in (3):

$$\mathbf{D}_1 = \frac{K_{IIC}}{K_{IC}}(\sqrt{\alpha_3}) \tag{36}$$

Therefore, the second form of modified maximum strain energy release rate criterion is given by:

$$K_I^2 + \left(\frac{\beta_1}{\mathbf{D}_1^2}\right)K_{II}^2 - K_{IC}^2 = 0 \tag{37}$$

and the damage factor in (37) is defined as:

$$\rho_{D_1} = \left(\frac{\beta_1}{D_1^2}\right) \tag{38}$$

The authors introduce $\rho_{D_1}$ as a "toughness damage factor". Substituting the toughness damage factor from (36) into (37) and doing necessary simplifications:

$$\left(\frac{K_I}{K_{IC}}\right)^2 + \left(\frac{K_{II}}{K_{IIC}}\right)^2 = 1 \tag{39}$$

Equation (39) is independent of elastic coefficients and material compliance matrix; therefore, it is not necessary to analyze the softening behavior of material in FPZ. In fact, by this approach, the damage compliance properties of material are replaced by material fracture properties, i.e. mode I and II fracture toughness, and as a consequence, we do not need to perform material nonlinear analysis.

## VI. Conclusion

Crack propagation in wood specimens includes creation of a

FPZ in the crack tip vicinity. The behavior of mechanical properties in this region is complicated and nonlinear due to microcrack formation and growth. In nearly all energy based proposed criteria for investigation of crack growth in wooden structures under mixed mode I/II, the nonlinear behavior of material and wasted energy due to microcrack growth is neglected by simplifying assumptions. Therefore, these criteria are too conservative in comparison with experimental data. In this article, wasted energy by microcracks in FPZ is considered by two different approaches:

1. Compliance Damage approach: Mechanical properties of damaged zone were calculated and maximum strain energy release rate criterion was modified by real FPZ properties. Therefore, the resultant fracture limit curves include the effects of microcrack wasted energy.
2. Toughness Damage approach: To avoiding complicated calculations, by definition of a suitable toughness damage factor, satisfying pure mode II condition, a simple method for estimation of compliance in FPZ was proposed. This factor makes the proposed criterion independent from material elastic and damage properties.

Verification was done using fracture experimental data for two kinds of softwood in RL direction, i.e. Scots pine [12] and Norway spruce [9]. Excellent compatibility with experimental data proved the accuracy of proposed methods.

## REFERENCES

[1] Smith, I. Landis, E. Gong, M. 2003. Fracture and Fatigue in Wood. Wiley Publisher.
[2] Romanowicz, M., Seweryn, A. 2008. Verification of a non-local stress criterion for mixed mode fracture in wood. Engineering Fracture Mechanics, Article in Press.
[3] Vasic, S. 2000. Application of fracture mechanics to wood. PhD Thesis. University of New Brunswick, Fredriction, NB, Canada.
[4] Mall, S., Murphy, J.E.1983. Criterion for mixed mode fracture in wood. Journal of Engineering Mechanics, 109(3):680-690.
[5] Wu, E.M.1976. Application of fracture mechanics to anisotropic plates. Journal of Applied Mechanics, 34(4): 967-974.
[6] Griffith, A. A.1921. The phenomena of rupture and flow in solids. Philosophical Transactions of the Royal Society of London, 221:163-197.
[7] Sih GC.1974. Strain-energy density factor applied to mixed mode crack problems. International Journal of Fracture, 10:305–21.
[8] Jernkvist L. O. 2001, Fracture of wood under mode loading I. Derivation of fracture criteria. Engineering fracture mechanics, 68:549-563.
[9] Jernkvist L. O. 2001, Fracture of wood under mode loading, II: Experimental investigation of picea abies. Engineering fracture mechanics, 68:565-576.
[10] Vasic, S. and Smith, I. 2002. Bridging crack model for fracture of spruce. Engineering Fracture Mechanics, 69: 745-760.
[11] Hillerborg, A., Modeer, M. and Petersson, P. E. 1976. Analysis of crack formation and crack growth in concrete by means of fracture mechanics and finite elements. Cement and Concrete research, 6: 773-782.
[12] Hunt D. G., Croager W. P. 1982. Mode II fracture toughness of wood measured by a mixed-mode test method. J Mat Sci Lett, 1: 77-79.
[13] USDA. 1999. Wood Handbook: Wood as an engineering material. Forest Products Laboratory, Forest Service, US Government Printing Office, Washington, DC,USA.
[14] Budiansky, B. O'Connell R. J. 1976. Elastic moduli of cracked solid. International Journal Solids Structures, 12: 81-97.